

Syntheses and Crystal Studies of Novel C-3'-N-sulfonyl and 7-O-acyl Modified Paclitaxel Analogues^①

XIAO Shang-Qing CUI Yong-Mei QIU Wei-Qing

CUI Ye-Sha LIN Hai-Xia^②

(Department of Chemistry, College of Sciences, Shanghai University, Shanghai 200444, China)

ABSTRACT Three C-3'-N-sulfonyl and C-7-O-acyl paclitaxel analogues were synthesized from 10-deacetyl baccatin III (10-DAB) and their structures were confirmed by ¹H NMR, ¹³C NMR and HR-MS. Among them, the crystal structure of compound **9b** was determined by single-crystal X-ray diffraction. Compound **9b** crystallizes in monoclinic system, space group *P*2₁ with *a* = 12.395(4), *b* = 15.215(5), *c* = 14.905(5) Å, *β* = 105.559(4)° and *Z* = 2. In the structure, the introduction of the hydrophobic 3-fluorobenzoyl group at C(7) has little effect on the conformation of tetracyclic system. However, the conformation of the side-chain at C(13) in **9b** is quite different from that of paclitaxel and docetaxel.

Keywords: paclitaxel, 3'-N-sulfonyl, crystal structure, bioactivity, conformation;

DOI: 10.14102/j.cnki.0254-5861.2011-3116

1 INTRODUCTION

Paclitaxel, a naturally occurring diterpenoid, isolated from the bark of Pacific yew (*Taxus brevifolia*) in 1971^[1], has shown remarkably high antitumor activity^[2]. Docetaxel^[3], a semisynthetic analogue, has also exhibited encouraging clinical usage and was approved by FDA for the treatment of breast cancer in 1996. Paclitaxel and docetaxel which act as promoters of tubulin assembly, as well as inhibitors of the disassembly process^[4,5], are two of the most important drugs currently used in the fight against various cancers, including breast, gastric, ovarian, and non-small cell lung carcinomas^[6-9].

An essential structural aspect related to the bioactivity of paclitaxel is the 3-D conformation of the drug. Structure activity relationship (SAR) studies have showed that the modification at C(7) is generally well tolerated^[10]. Benzoyl derivatives^[11, 12] bearing modification at C(7) have all been prepared and found to have good activities in the microtubule assembly assay. The effects of C(7) modification can also be seen from the cabazitaxel^[13]. SAR studies so far indicate that the C(13) side chain is essential for antitumor activity. This fact is proved by the binding conformation of paclitaxel in

β-tubulin^[14]. Therefore, understanding the 3-D structures of this series of active or inactive compounds is very important for further design and synthesis of improved anticancer agents. A large number of 3'-N-acyl analogues have been studied, but SAR studies on 3'-N-sulfonyl analogues have received little attention. Only a few C-3'-N-sulfonyl analogues^[15] have been reported, and their biological test results showed potent cytotoxicities against human tumor cell lines Eca-109, SKOV3, SMMC-7721, HCT-8, PC3, MCF-7, HeLa and KB. Herein, we report the preparation of three paclitaxel analogues with different sulfonyl substituted groups at the C-3'-N position and modification at the C(7) position, starting from 10-deacetyl baccatin III. Also, the crystal structure of **9b** was reported.

2 EXPERIMENTAL

2.1 Materials and methods

Unless otherwise noted, all chemicals and solvents were commercial reagent grade and used without further purification. All reported yields are obtained after column chromatography or crystallization. ¹H NMR and ¹³C NMR spectra were recorded on a Bruker DM-500MHz spectro-

Received 25 January 2021; accepted 20 April 2021 (CCDC 1905148)

① The project was supported by the National Natural Science Foundation of China (Nos. 21272154 and 81202402)

② Corresponding author. E-mail: haixialin@staff.shu.edu.cn

meter at 500.134 and 125.771 MHz, respectively, with TMS as an internal standard. Mass spectra were recorded using an ESI source (Agilent 6320 instrument). All chemicals were dried or purified according to standard procedures prior to use.

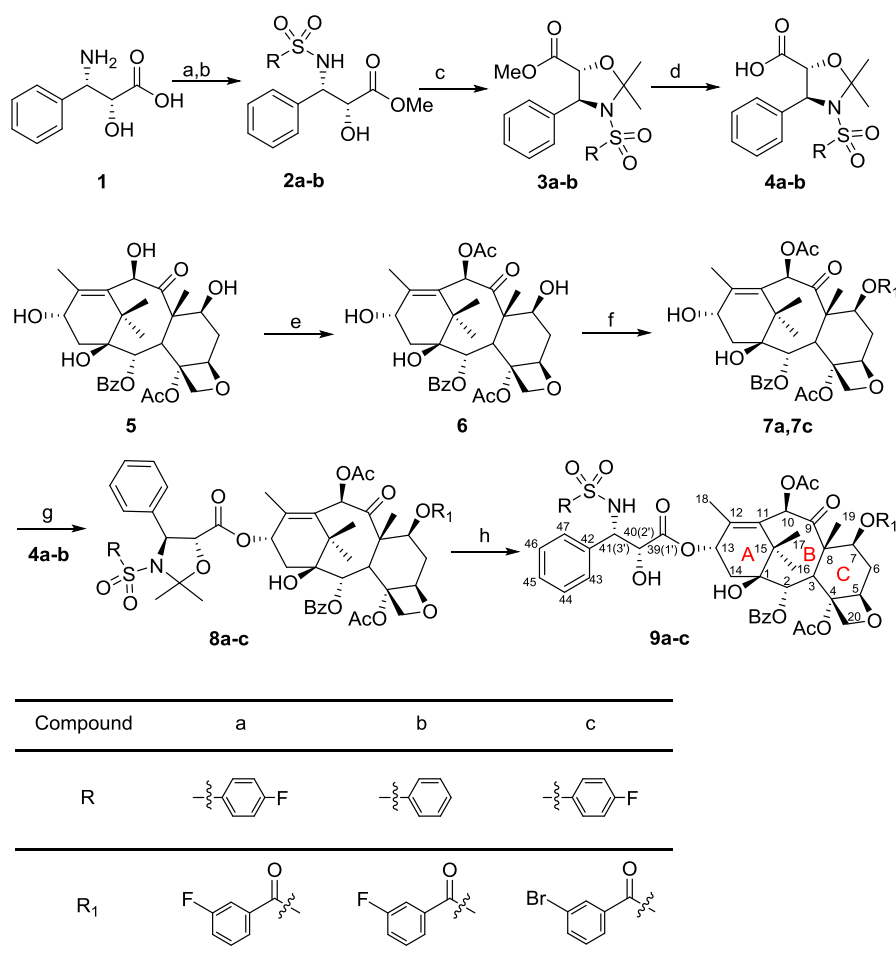
2.2 Routes for the syntheses of the target compounds

Acylation catalyzed by CeCl_3 with acetic anhydride at room temperature took place preferentially at C-10-OH of 10-DAB to form **6**^[10]. Treatment of **6** with acyl chloride in the presence of Et_3N and 4-dimethylaminopyridine (DMAP) in toluene at 50 °C afforded compounds **7a** and **7c**. Then the corresponding side chain carboxylic acids **4a~b**^[16] were coupled with compounds **7a** and **7c** in the presence of dicyclohexylcarbodiimide (DCC) and DMAP at 50 °C to provide the corresponding cyclic ester intermediates **8a~c** in 85~95% yields. The target products **9a~c** were obtained after hydrolysis of the acetonide protecting groups.

2.3 Syntheses of compounds 2a~b

To a solution of (2*R*, 3*S*)-3-phenylisoserine **1** (100 mg,

0.52 mmol) in anhydrous MeOH (3 mL), thionyl chloride (SOCl_2 , 0.05 mL, 0.79 mmol) was added dropwise at 0 °C. The reaction mixture was stirred overnight at room temperature. The reaction was quenched with NaHCO_3 and the solution was evaporated under reduced pressure and diluted with H_2O . The water phase was extracted with EtOAc, and the combined organic layer was dried over anhydrous Na_2SO_4 and concentrated. Subsequently, to a solution of the previous product in a mixture of THF (10 mL) and saturated NaHCO_3 (10 mL), one of a series of different sulfonyl chlorides (3 mmol) was added dropwise at 0 °C, respectively. The whole mixture was stirred vigorously at room temperature for 2 h. THF was distilled under reduced pressure. The desired compounds were extracted with EtOAc, dried over anhydrous Na_2SO_4 , concentrated, and purified by silica gel column chromatography (petroleum ether:EtOAc = 2:1), yielding products **2a~b** as a white solid.



Scheme 1. Reagents and conditions: (a) SOCl_2 , MeOH, 0 °C to rt.; (b) sulfonyl chloride, THF, sat. NaHCO_3 , 0 °C to rt., 80~90%; (c) 2-methoxypropene, PPTS, toluene, 90 °C, 80~90%; (d) KOH, MeOH, rt.; (e) acetic anhydride, CeCl_3 , THF, rt., 70%; (f) Et_3N , DMAP, acyl chloride, toluene, 50 °C, 80~85%; (g) **4a-b**, DCC, DMAP, toluene, 50 °C, 85~95%; (h) formic acid, rt., 28~35%

Compound 2a: white solid, yield 84%. ^1H NMR (500 MHz, CDCl_3) δ (ppm): 3.38 (d, $J = 8.5$ Hz, 1H), 3.81 (s, 3H), 4.36 (dd, $J = 2.1, 6.7$ Hz, 1H), 4.86 (dd, $J = 7.7, 12.0$ Hz, 1H), 5.87 (d, $J = 4.9$ Hz, 1H), 6.90~6.94 (m, 2H), 7.09~7.11 (m, 2H), 7.17 (d, $J = 1.7$ Hz, 2H), 7.38~7.43 (m, 1H), 7.61 (dd, $J = 3.8, 13.9$ Hz, 2H); ^{13}C NMR (125 MHz, CDCl_3) δ (ppm): 53.2, 59.5, 74.5, 115.7, 115.9, 127.0, 127.9, 128.4, 129.7, 129.7, 136.5, 136.6, 136.9, 163.7, 165.8, 172.6.

Compound 2b: white solid, yield 89%. ^1H NMR (500 MHz, CDCl_3) δ (ppm): 3.72 (br, 1H), 3.82 (s, 3H), 4.42 (br, 1H), 4.94 (dd, $J = 7.7, 11.9$ Hz, 1H), 6.01 (d, $J = 9.8$ Hz, 1H), 7.07~7.11 (m, 1H), 7.34 (t, $J = 7.0$ Hz, 3H), 7.46 (t, $J = 7.5$ Hz, 1H), 7.58~7.64 (m, 1H), 7.71 (d, $J = 7.4$ Hz, 2H), 7.71 (d, $J = 7.4$ Hz, 2H); ^{13}C NMR (125 MHz, CDCl_3) δ (ppm): 53.1, 59.5, 74.5, 125.9, 126.1, 126.9, 127.0, 127.8, 128.3, 128.7, 128.9, 129.3, 132.3, 137.2, 140.5, 172.6.

2.4 Syntheses of compounds 3a~b

To a solution of compounds **2a~b** (1 mmol) and pyridinium *p*-toluenesulfonate (PPTS) (0.1 mmol) in anhydrous toluene (30 mL), 2-methoxypropene (3 mmol) was subsequently added dropwise under nitrogen atmosphere. The reaction mixture was stirred at 90~100 °C for 3 h. After cooling down to room temperature, the mixture was diluted with EtOAc. The organic layer was washed with brine, and dried over anhydrous Na_2SO_4 . The solvent was evaporated after filtering and the residue was purified by silica gel column chromatography (petroleum ether:EtOAc = 5:1), yielding products **3a~b** as a yellow oil.

Compound 3a: yellow oil, yield 86%. ^1H NMR (500 MHz, CDCl_3) δ (ppm): 1.76 (s, 3H), 1.84 (s, 3H), 3.67 (s, 3H), 4.47 (d, $J = 5.3$ Hz, 1H), 5.15 (d, $J = 5.3$ Hz, 1H), 6.84 (t, $J = 8.5$ Hz, 2H), 7.09~7.14 (m, 5H), 7.40 (dd, $J = 3.7, 13.8$ Hz, 2H). ^{13}C NMR (125 MHz, CDCl_3) δ (ppm): 27.1, 28.6, 52.6, 65.1, 81.8, 100.7, 115.4, 115.6, 127.8, 128.2, 128.5, 130.2, 130.2, 136.9, 137.0, 137.3, 163.6, 165.7, 170.3.

Compound 3b: yellow oil, yield 84%. ^1H NMR (500 MHz, CDCl_3) δ (ppm): 1.81 (s, 3H), 1.89 (s, 3H), 3.70 (s, 3H), 4.53 (d, $J = 5.2$ Hz, 1H), 5.23 (d, $J = 5.3$ Hz, 1H), 7.13~7.17 (m, 3H), 7.21~7.24 (m, 4H), 7.37~7.40 (m, 1H), 7.49 (t, $J = 7.4$ Hz, 2H); ^{13}C NMR (125 MHz, CDCl_3) δ (ppm): 27.0, 28.8, 52.6, 65.2, 81.7, 102.6, 115.4, 115.6, 127.4, 128.1, 128.3, 130.1, 130.2, 136.9, 137.0, 137.3, 139.7, 140.7, 170.4.

2.5 Syntheses of compounds 7a and 7c

To a solution of compound **6** (96 mg, 0.12 mmol) in anhydrous toluene (5 mL), 3-fluorobenzoyl chloride (0.24 mmol) or 3-bromobenzoyl chloride (0.24 mmol) and DMAP

(0.12 mmol) were added. The reaction mixture was stirred for 0.5 h at room temperature, and then quenched with saturated NaHCO_3 (2 mL), diluted with EtOAc (30 mL) and washed with water and brine. The organic layer was dried over anhydrous Na_2SO_4 and the crude products were purified by silica gel column chromatography (petroleum ether:EtOAc = 1:1), yielding **7a** and **7c** as a white solid.

Compound 7a: white solid, yield 82%. ^1H NMR (500 MHz, CDCl_3) δ (ppm): 1.09 (s, 3H), 1.16 (s, 3H), 1.81 (s, 1H), 1.93 (d, $J = 3.5$ Hz, 1H), 1.95 (s, 3H), 2.01 (s, 3H), 2.06 (s, 3H), 2.14 (s, 3H), 2.77~2.83 (m, 1H), 4.10 (d, $J = 6.1$ Hz, 1H), 4.21 (d, $J = 8.4$ Hz, 1H), 4.37 (d, $J = 8.4$ Hz, 1H), 4.88 (t, $J = 7.7$ Hz, 1H), 5.03 (d, $J = 9.0$ Hz, 1H), 5.70 (d, $J = 6.9$ Hz, 1H), 5.79 (dd, $J = 7.3, 10.4$ Hz, 1H), 6.40 (s, 1H), 7.30 (t, $J = 7.2$ Hz, 1H), 7.38~7.42 (m, 1H), 7.50 (t, $J = 7.6$ Hz, 2H), 7.60~7.64 (m, 2H), 7.72 (d, $J = 7.7$ Hz, 1H), 8.13 (d, $J = 6.5$ Hz, 2H); ^{13}C NMR (125 MHz, CDCl_3) δ (ppm): 10.9, 15.2, 20.2, 20.5, 22.5, 26.6, 33.3, 38.5, 42.7, 47.2, 56.3, 67.8, 72.8, 74.5, 75.5, 76.4, 78.7, 80.5, 83.9, 116.8, 119.9, 122.1, 125.5, 128.7, 129.3, 129.8, 130.1, 131.7, 132.2, 132.8, 133.7, 135.7, 144.9, 164.2, 167.1, 168.6, 170.7, 202.9. HR-MS: calcd. for $\text{C}_{38}\text{H}_{41}\text{FO}_{12}$ ($[\text{M} + \text{H}]^+$), 709.7331, found 709.7320.

Compound 7c: white solid, yield 83%. ^1H NMR (500 MHz, CDCl_3) δ (ppm): 1.09 (s, 3H), 1.16 (s, 3H), 1.78 (s, 1H), 1.90 (d, $J = 2.5$ Hz, 1H), 1.94 (s, 3H), 2.02 (s, 3H), 2.06 (s, 3H), 2.14 (s, 3H), 2.48 (s, 1H), 2.76~2.83 (m, 1H), 4.10 (d, $J = 8.0$ Hz, 1H), 4.21 (d, $J = 8.5$ Hz, 1H), 4.37 (d, $J = 8.5$ Hz, 1H), 4.88 (t, $J = 7.2$ Hz, 1H), 5.03 (d, $J = 8.6$ Hz, 1H), 5.70 (d, $J = 6.9$ Hz, 1H), 5.79 (dd, $J = 7.2, 10.4$ Hz, 1H), 6.40 (s, 1H), 7.30 (t, $J = 8.2$ Hz, 1H), 7.51 (t, $J = 7.7$ Hz, 2H), 7.63 (t, $J = 7.4$ Hz, 1H), 7.66~7.68 (m, 1H), 7.84 (d, $J = 7.8$ Hz, 1H), 8.04 (s, 1H), 8.13 (d, $J = 7.2$ Hz, 2H); ^{13}C NMR (125 MHz, CDCl_3) δ (ppm): 10.9, 15.2, 20.2, 20.5, 22.6, 26.6, 33.3, 38.5, 42.8, 47.2, 56.3, 67.8, 72.8, 74.4, 75.4, 76.4, 78.7, 80.6, 83.9, 116.8, 119.9, 122.1, 128.4, 128.7, 129.3, 129.7, 130.1, 131.8, 132.2, 132.8, 133.8, 135.7, 144.9, 164.2, 167.1, 168.6, 170.7, 202.9. HR-MS: calcd. for $\text{C}_{38}\text{H}_{41}\text{BrO}_{12}$ ($[\text{M} + \text{H}]^+$), 770.6387, found 770.6375.

2.6 Syntheses of compounds 8a~c

To a solution of compounds **3a~b** (1 mmol) in MeOH, a solution of KOH (1.2 mmol) in water (4 mL) was added slowly at room temperature. The reaction mixture was stirred for 1.5 h. After the completion of the reaction, MeOH was evaporated under reduced pressure. The residual mixture was successively diluted with water, washed with Et_2O , acidified with 3 N HCl, and extracted with EtOAc. The organic phase

was dried over Na_2SO_4 and evaporated under reduced pressure. The resulting crude products (2.0 mmol), compounds **7a**, **7c** (1.0 mmol), DCC (2.0 mmol) and DMAP (1.0 mmol) were dissolved in anhydrous toluene (6 mL), and the reaction mixture was stirred for 2 h at 50 °C. The reaction mixture was diluted with EtOAc, and washed with water and brine. The organic layer was dried over anhydrous Na_2SO_4 and the crude products were purified by silica gel column chromatography (petroleum ether:EtOAc = 2:1), yielding products **8a~c** as white solid.

Compound 8a: white solid, yield 87%. ^1H NMR (500 MHz, CDCl_3) δ (ppm): 1.18 (s, 3H), 1.20 (s, 3H), 1.41~1.46 (m, 3H), 1.67~1.73 (m, 3H), 1.86 (s, 3H), 1.95 (s, 3H), 2.00 (s, 3H), 2.16~2.28 (m, 2H), 2.34 (s, 3H), 2.73~2.80 (m, 1H), 3.97 (d, J = 6.9 Hz, 1H), 4.24 (d, J = 8.3 Hz, 1H), 4.54 (d, J = 3.0 Hz, 1H), 4.98 (t, J = 9.7 Hz, 2H), 5.70 (t, J = 7.0 Hz, 2H), 6.01 (br, 1H), 6.14 (t, J = 8.8 Hz, 1H), 6.33 (s, 1H), 6.91 (t, J = 8.5 Hz, 2H), 7.11 (d, J = 3.7 Hz, 2H), 7.20 (d, J = 3.9 Hz, 3H), 7.37~7.41 (m, 1H), 7.49 (t, J = 7.6 Hz, 2H), 7.52~7.62 (m, 4H), 7.69~7.72 (m, 2H), 8.09 (d, J = 7.3 Hz, 2H); ^{13}C NMR (125 MHz, CDCl_3) δ (ppm): 11.0, 14.7, 20.4, 21.2, 21.6, 24.9, 25.6, 26.3, 27.2, 28.6, 33.2, 33.9, 35.6, 43.2, 46.7, 49.1, 56.1, 65.2, 71.7, 72.4, 74.6, 74.7, 76.2, 78.9, 80.5, 82.1, 83.9, 101.1, 115.5, 115.7, 116.6, 116.7, 119.8, 119.9, 125.5, 125.6, 128.1, 128.4, 128.6, 128.7, 129.1, 130.1, 130.2, 130.3, 133.1, 133.8, 136.8, 140.8, 163.3, 163.7, 164.2, 166.9, 168.4, 169.8, 169.9, 202.3.

Compound 8b: white solid, yield 89%. ^1H NMR (500 MHz, CDCl_3) δ (ppm): 1.14 (s, 3H), 1.18 (s, 3H), 1.85 (s, 3H), 1.88 (s, 3H), 1.90~1.95 (m, 9H), 1.97 (s, 3H), 2.01 (d, J = 3.9 Hz, 2H), 2.10~2.16 (m, 2H), 2.68~2.75 (m, 1H), 3.96 (d, J = 6.9 Hz, 1H), 4.07~4.15 (m, 1H), 4.26 (d, J = 8.5 Hz, 1H), 4.49 (d, J = 6.2 Hz, 1H), 4.92 (d, J = 9.3 Hz, 1H), 5.21 (d, J = 6.2 Hz, 1H), 5.67 (d, J = 6.9 Hz, 1H), 5.71~5.74 (m, 1H), 6.17 (t, J = 8.7 Hz, 1H), 6.34 (br, 1H), 7.14 (t, J = 7.5 Hz, 2H), 7.19~7.25 (m, 6H), 7.37 (t, J = 5.6 Hz, 2H), 7.44~7.47 (m, 4H), 7.59 (dd, J = 6.9, 21.9 Hz, 2H), 7.70 (d, J = 7.5 Hz, 1H), 8.01 (d, J = 7.7 Hz, 2H); ^{13}C NMR (125 MHz, CDCl_3) δ (ppm): 11.0, 14.7, 20.4, 21.2, 21.6, 26.2, 27.1, 28.7, 33.2, 33.8, 35.5, 43.2, 46.7, 53.5, 56.0, 65.3, 71.6, 72.4, 74.5, 74.7, 76.2, 78.9, 80.5, 81.9, 83.8, 100.9, 116.5, 116.7, 119.8, 119.9, 125.5, 125.6, 127.4, 127.9, 128.3, 128.5, 128.6, 128.7, 129.1, 129.7, 129.8, 130.0, 132.4, 133.0, 133.8, 137.0, 140.5, 140.8, 161.3, 163.3, 164.2, 166.8, 168.5, 169.8, 169.9, 202.3.

Compound 8c: white solid, yield 92%. ^1H NMR (500 MHz, CDCl_3) δ (ppm): 1.14 (s, 3H), 1.19 (s, 3H), 1.87 (s,

3H), 1.89 (s, 3H), 1.92 (s, 2H), 1.94 (s, 3H), 1.99 (s, 6H), 2.01 (s, 3H), 2.14~2.17 (m, 2H), 2.69~2.75 (m, 1H), 3.98 (d, J = 7.0 Hz, 1H), 4.14 (d, J = 8.5 Hz, 1H), 4.27 (d, J = 8.5 Hz, 1H), 4.54 (d, J = 6.2 Hz, 1H), 4.93 (d, J = 9.0 Hz, 1H), 5.24 (d, J = 6.1 Hz, 1H), 5.67 (d, J = 7.0 Hz, 1H), 5.73 (t, J = 3.3 Hz, 1H), 6.19 (t, J = 8.4 Hz, 1H), 6.35 (br, 1H), 6.95 (t, J = 6.2 Hz, 2H), 7.08~7.13 (m, 1H), 7.17~7.22 (m, 6H), 7.27 (t, J = 7.7 Hz, 2H), 7.45 (t, J = 7.8 Hz, 2H), 7.59 (t, J = 7.4 Hz, 1H), 7.64 (dd, J = 7.2, 8.7 Hz, 1H), 7.83 (d, J = 7.8 Hz, 1H), 8.01 (d, J = 7.6 Hz, 3H); ^{13}C NMR (125 MHz, CDCl_3) δ (ppm): 11.1, 14.1, 14.7, 20.5, 21.2, 21.6, 24.9, 25.6, 26.2, 27.1, 28.7, 29.7, 33.1, 33.9, 35.3, 43.2, 46.7, 56.1, 65.3, 71.6, 72.5, 74.5, 74.7, 76.3, 78.9, 80.5, 81.9, 83.9, 100.9, 122.1, 127.5, 127.9, 128.3, 128.4, 128.5, 128.6, 128.7, 129.1, 129.7, 130.1, 132.4, 132.8, 132.9, 133.8, 135.8, 137.1, 140.6, 140.9, 156.8, 164.1, 166.9, 168.5, 169.8, 169.9, 202.3.

2.7 Syntheses of compounds 9a~c

HCOOH (>98%, 5 mL) was added to compounds **8a~c**, and the reaction mixture was stirred at room temperature for 4 h. Then the resulting solution was neutralized by adding saturated NaHCO_3 . After extracting with EtOAc, the combined organic phase was washed with brine and dried over anhydrous Na_2SO_4 . The crude products were purified by thin layer chromatography, yielding products **9a~c** as white solid.

Compound 9a: white solid, yield 31%. m.p.: 120~121 °C. ^1H NMR (500 MHz, CDCl_3) δ (ppm): 1.17 (s, 3H), 1.19 (s, 3H), 1.85 (s, 3H), 1.95 (s, 3H), 1.99 (s, 3H), 2.04 (s, 2H), 2.22~2.30 (m, 2H), 2.35 (s, 3H), 2.71~2.77 (m, 1H), 3.87 (br, 1H), 3.96 (d, J = 6.8 Hz, 1H), 4.25 (d, J = 8.4 Hz, 1H), 4.32 (d, J = 9.0 Hz, 1H), 4.54 (d, J = 2.4 Hz, 1H), 4.93~4.97 (m, 2H), 5.70 (t, J = 6.9 Hz, 2H), 6.16 (t, J = 8.6 Hz, 1H), 6.21 (d, J = 8.5 Hz, 1H), 6.32 (s, 1H), 6.88 (t, J = 8.4 Hz, 2H), 7.10 (d, J = 3.5 Hz, 2H), 7.17 (t, J = 3.6 Hz, 3H), 7.23~7.26 (m, 1H), 7.36~7.40 (m, 1H), 7.47 (t, J = 7.7 Hz, 2H), 7.58 (t, J = 6.8 Hz, 4H), 7.70 (d, J = 7.7 Hz, 1H), 8.09 (d, J = 7.3 Hz, 2H); ^{13}C NMR (125 MHz, CDCl_3) δ (ppm): 11.0, 14.7, 20.4, 20.9, 22.4, 26.4, 33.2, 35.7, 43.1, 46.7, 56.2, 59.7, 72.0, 72.5, 74.4, 74.6, 74.7, 76.3, 78.6, 81.0, 83.7, 115.7, 115.9, 116.5, 116.7, 119.9, 120.0, 125.4, 125.5, 127.1, 128.3, 128.5, 129.1, 129.6, 129.7, 130.1, 132.1, 133.2, 133.8, 136.1, 136.3, 140.3, 161.3, 163.2, 163.7, 164.0, 164.3, 165.8, 166.8, 168.5, 170.6, 171.2, 202.2. HR-MS: calcd. for $\text{C}_{53}\text{H}_{53}\text{F}_2\text{NO}_{16}\text{S}$ ($[\text{M} + \text{H}]^+$), 1030.3131, found 1030.3119.

Compound 9b: white solid, yield 28%. m.p.: 135~136 °C. ^1H NMR (500 MHz, CDCl_3) δ (ppm): 1.16 (s, 3H), 1.18 (s,

3H), 1.86 (s, 3H), 1.94 (s, 3H), 1.97 (s, 3H), 2.15~2.21 (m, 2H), 2.25 (d, $J = 8.9$ Hz, 2H), 2.36 (s, 3H), 2.70~2.77 (m, 1H), 3.96 (d, $J = 6.8$ Hz, 2H), 4.28 (dd, $J = 19.2, 36.4$ Hz, 2H), 4.52 (br, 1H), 4.90 (dd, $J = 6.0, 12.5$ Hz, 1H), 4.95 (d, $J = 9.3$ Hz, 1H), 5.70 (t, $J = 7.1$ Hz, 2H), 6.17 (t, $J = 8.7$ Hz, 1H), 6.32 (s, 2H), 7.07 (t, $J = 1.9$ Hz, 2H), 7.12 (d, $J = 2.9$ Hz, 3H), 7.22 (t, $J = 7.9$ Hz, 3H), 7.35~7.38 (m, 2H), 7.46 (t, $J = 7.7$ Hz, 2H), 7.59 (d, $J = 7.3$ Hz, 4H), 7.69 (d, $J = 7.7$ Hz, 1H), 8.09 (d, $J = 7.3$ Hz, 2H); ^{13}C NMR (125 MHz, CDCl_3) δ (ppm): 11.1, 14.2, 14.7, 20.5, 21.0, 21.1, 22.5, 26.4, 33.2, 35.8, 43.1, 46.7, 56.2, 59.7, 60.5, 72.1, 72.5, 74.5, 74.6, 74.7, 78.7, 80.9, 83.8, 116.6, 116.8, 119.8, 120.0, 125.5, 125.6, 126.9, 127.1, 128.2, 128.5, 128.6, 128.7, 129.2, 130.1, 132.5, 133.2, 133.8, 136.3, 140.2, 140.5, 161.3, 163.3, 164.2, 164.3, 166.8, 168.5, 170.5, 171.3, 171.5, 202.4. HR-MS: calcd. for $\text{C}_{53}\text{H}_{54}\text{FNO}_{16}\text{S}$ ($[\text{M} + \text{H}]^+$), 1012.3225, found 1012.3210.

Compound 9c: white solid, yield 34%. m.p.: 125~126 °C. ^1H NMR (500 MHz, CDCl_3) δ (ppm): 1.17 (s, 3H), 1.20 (s, 3H), 1.86 (s, 3H), 1.94 (s, 3H), 2.00 (s, 3H), 2.12~2.30 (m, 4H), 2.36 (s, 3H), 2.71~2.77 (m, 1H), 3.96 (d, $J = 6.8$ Hz, 1H), 4.24 (d, $J = 8.5$ Hz, 1H), 4.31 (t, $J = 4.0$ Hz, 2H), 4.53 (d, $J = 2.7$ Hz, 1H), 4.94 (dd, $J = 9.9, 22.9$ Hz, 2H), 5.67~5.71 (m, 2H), 6.16 (t, $J = 8.6$ Hz, 1H), 6.37 (d, $J = 9.2$ Hz, 1H), 6.88 (t, $J = 8.4$ Hz, 2H), 7.10 (d, $J = 3.6$ Hz, 2H), 7.17 (d, $J = 3.2$ Hz, 3H), 7.27 (dd, $J = 7.9, 19.2$ Hz, 1H), 7.47 (t, $J = 7.6$ Hz, 2H), 7.59 (dd, $J = 7.3, 20.7$ Hz, 3H), 7.65 (d, $J = 7.9$ Hz, 1H), 7.82 (d, $J = 7.7$ Hz, 1H), 8.01 (s, 1H), 8.09 (d, $J = 7.5$ Hz, 2H); ^{13}C NMR (125 MHz, CDCl_3) δ (ppm): 11.1, 14.1, 14.8, 19.2, 20.5, 20.7, 20.9, 22.5, 22.7, 26.5, 29.1, 29.4, 29.7, 30.6, 31.9, 33.3, 35.7, 43.1, 46.8, 56.3, 59.8, 62.3, 65.6, 72.0, 72.6, 74.4, 74.8, 76.4, 78.7, 81.1, 83.8, 115.8, 115.9, 122.2,

127.2, 126.6, 128.7, 129.6, 129.7, 129.8, 130.1, 130.9, 132.0, 132.8, 135.9, 136.2, 140.4, 164.2, 166.9, 168.6, 170.6, 171.2, 202.3. HR-MS: calcd. for $\text{C}_{53}\text{H}_{53}\text{BrFNO}_{16}\text{S}$ ($[\text{M} + \text{H}]^+$), 1090.2331, found 1090.2325.

2.8 Crystal structure determination of 9b

Monocrystal of **9b** suitable for X-ray analysis was grown by slow evaporation of methanol at room temperature. The selected crystal (0.16mm \times 0.12mm \times 0.10mm) was mounted on a Bruker APEX-II CCD diffractometer. Diffraction data were measured at 296(2) K using graphite-monochromated Mo- $K\alpha$ ($\lambda = 0.71073$ Å) radiation. A total of 14111 reflections were collected in the range of $1.95 \leq \theta \leq 25.05^\circ$ ($-13 \leq h \leq 14$, $-18 \leq k \leq 11$, $-17 \leq l \leq 16$), of which 6952 were independent ($R_{\text{int}} = 0.0385$) and 4908 were observed with $I > 2\sigma(I)$. The structure was solved by direct methods and refined by full-matrix least-squares method on F^2 by using the SHELXTL software package. All non-H atoms were anisotropically refined. The hydrogen atoms were located by geometry calculation and riding on the related parent atoms. Crystal data for **9b**: monoclinic system, space group $P2_1$ with $a = 12.395(4)$, $b = 15.215(5)$, $c = 14.905(5)$ Å, $\beta = 105.559(4)^\circ$, $V = 2707.9(16)$ Å³, $Z = 2$, $\text{C}_{53}\text{H}_{53}\text{FNO}_{16}\text{S}$, $M_r = 1011.02$, $D_c = 1.240$ Mg/m³, $F(000) = 1100$. The final $R = 0.0524$, $wR = 0.1298$ ($w = 1/[\sigma^2(F_o^2) + (0.0869P)^2 + 0.1686P]$, where $P = (F_o^2 + 2F_c^2)/3$), and $R = 0.0817$, $wR = 0.1516$ for all data. The goodness-of-fit on F^2 was 1.002. The maximum and minimum peaks are 0.313 and -0.216 e/Å³, respectively. Selected bond distances and bond angles are listed in Tables 1 and 2. The structure of molecule **9b** with atomic labeling is shown in Fig. 1. A view of the crystal packing along the a -axis is shown in Fig. 2.

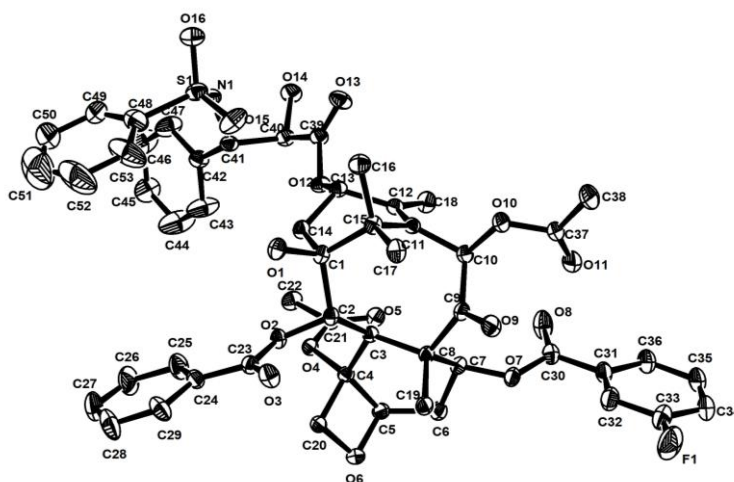


Fig. 1. Molecular structure with labeling scheme of **9b**

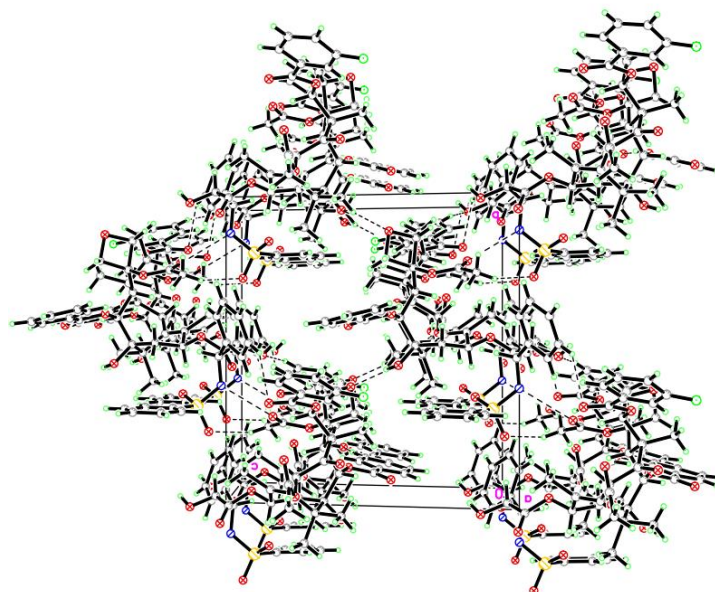
Fig. 2. A view of the crystal packing along the *a*-axis

Table 1. Selected Bond Lengths (Å) for Compound 9b

Bond	Dist.	Bond	Dist.	Bond	Dist.
C(1)–O(1)	1.429(6)	C(11)–C(15)	1.530(7)	C(4)–O(4)	1.448(6)
C(1)–C(14)	1.541(7)	C(12)–C(13)	1.510(7)	C(4)–C(20)	1.532(7)
C(1)–C(15)	1.558(7)	C(12)–C(18)	1.517(8)	C(4)–C(5)	1.550(8)
C(1)–C(2)	1.572(8)	C(13)–O(12)	1.464(6)	C(5)–O(6)	1.455(8)
C(2)–O(2)	1.459(6)	C(13)–C(14)	1.533(8)	C(5)–C(6)	1.508(8)
C(2)–C(3)	1.559(7)	C(15)–C(17)	1.544(8)	C(6)–C(7)	1.494(8)
C(3)–C(4)	1.544(7)	C(15)–C(16)	1.565(9)	C(7)–O(7)	1.450(6)
C(3)–C(8)	1.576(6)	C(20)–O(6)	1.445(7)	C(7)–C(8)	1.549(8)
C(8)–C(19)	1.542(7)	C(9)–C(10)	1.529(8)	C(11)–C(12)	1.340(7)
C(8)–C(9)	1.560(7)	C(10)–O(10)	1.444(6)	C(39)–C(40)	1.515(8)
C(9)–O(9)	1.207(6)	C(10)–C(11)	1.501(8)	C(39)–O(13)	1.200(7)
C(40)–C(41)	1.546(8)	C(41)–C(42)	1.550(1)	C(40)–O(14)	1.415(6)

Table 2. Selected Angles (°) for Compound 9b

Angle	(°)	Angle	(°)	Angle	(°)
O(1)–C(1)–C(14)	105.6(4)	O(10)–C(10)–C(9)	108.9(4)	C(10)–C(9)–C(8)	120.8(4)
O(10)–C(10)–C(11)	108.4(5)	C(11)–C(10)–C(9)	113.9(4)	O(7)–C(7)–C(8)	107.1(4)
C(14)–C(1)–C(15)	111.1(4)	C(12)–C(11)–C(10)	121.1(5)	C(6)–C(7)–C(8)	114.2(4)
O(1)–C(1)–C(2)	106.5(4)	C(12)–C(11)–C(15)	118.8(5)	O(9)–C(9)–C(8)	119.3(5)
C(14)–C(1)–C(2)	110.9(4)	C(10)–C(11)–C(15)	119.8(4)	C(19)–C(8)–C(9)	107.0(4)
C(15)–C(1)–C(2)	111.1(4)	C(11)–C(12)–C(13)	116.6(5)	C(7)–C(8)–C(9)	104.2(4)
O(2)–C(2)–C(3)	108.1(4)	C(11)–C(12)–C(18)	126.0(5)	C(19)–C(8)–C(3)	113.4(4)
O(2)–C(2)–C(1)	104.6(4)	C(13)–C(12)–C(18)	117.4(5)	C(7)–C(8)–C(3)	105.8(4)
C(3)–C(2)–C(1)	119.1(4)	O(12)–C(13)–C(12)	113.5(4)	C(9)–C(8)–C(3)	115.5(4)
C(4)–C(3)–C(2)	112.6(4)	O(12)–C(13)–C(14)	104.8(4)	C(6)–C(5)–C(4)	119.4(5)
C(4)–C(3)–C(8)	111.6(4)	C(12)–C(13)–C(14)	111.0(4)	C(7)–C(6)–C(5)	114.3(5)
C(2)–C(3)–C(8)	114.1(4)	C(1)–C(14)–C(13)	114.9(4)	C(39)–C(40)–C(41)	109.3(5)
O(4)–C(4)–C(20)	108.1(4)	C(11)–C(15)–C(17)	115.9(6)	C(42)–C(41)–C(40)	112.3(5)
O(4)–C(4)–C(3)	109.4(4)	C(11)–C(15)–C(1)	105.8(4)	O(13)–C(39)–O(12)	124.7(6)
C(20)–C(4)–C(3)	120.9(4)	C(17)–C(15)–C(1)	111.1(4)	O(13)–C(39)–C(40)	125.8(6)
O(4)–C(4)–C(5)	111.5(4)	C(11)–C(15)–C(16)	110.4(4)	O(12)–C(39)–C(40)	109.4(5)
C(20)–C(4)–C(5)	85.3(4)	C(17)–C(15)–C(16)	103.9(5)	O(14)–C(40)–C(41)	109.6(6)
C(3)–C(4)–C(5)	119.6(4)	C(1)–C(15)–C(16)	110.3(5)	O(14)–C(40)–C(39)	110.0(5)

3 RESULTS AND DISCUSSION

The cyclooctane ring B adopts the most stable boat-chair conformation, as shown by the torsion angles with atoms C(1) and C(9) as the ends. This ring is transfused along the C(3)–C(8) bond to the six-membered ring C, which exhibits a chair conformation flattened in C(4) (atoms C(7) and C(4) deviated by -0.653 and 0.191 Å, respectively from the mean plane of the other four atoms). Ring A, “double-bridged” to the central ring, exhibits a boat conformation with C(13) only 0.525 Å and C(15) 0.690 Å fully above the mean plane of atoms C(11), C(12), C(14), and C(1). The diterpenoid core of **9b** is similar to the diterpenoid core of paclitaxel^[17], and other baccatin derivatives such as baccatin III^[18] and 1-deoxybaccatin VI^[19].

Structure activity relationship studies so far indicate that the C(13) side chain is essential for antitumor activity. The stereochemistry of the side chain at C(2') and C(3') is crucial for biological activity^[20]. For a more detailed comparison of the C(13) side chain conformations, selected torsion angles for **9b**, paclitaxel, docetaxel and T-Taxol are listed in Table 3. Comparing the solid-state conformation of **9b** with that of

paclitaxels A and B, three corresponding torsion angles differ by nearly 100° (C(1')–C(2')–C(3')–N, O(14)–C(2')–C(3')–C(39), C(3')–N–S(C)–C(45)). When compared with the solid-state conformation of docetaxel and T-Taxol, three corresponding torsion angles differ by more than 31° (C(2')–C(3')–N–S(C), C(39)–C(3')–N–S(C), C(3')–N–S(C)–C(45)). The variations in torsion angles around the C(1')–C(2') and C(2')–C(3') bonds seem to dominate changes in the orientation of the side chain relative to the core. The comparison of torsion angles shows that the conformation of C(13) side chain of **9b** is significantly different from that of the solid conformation of paclitaxel, docetaxel and T-Taxol. As shown by the superposition of the crystal conformers (Fig. 3), although **9b** has a 3-fluorobenzoyl group at C(7) instead of a hydroxyl group in paclitaxel, the conformation of the common part of the tetracyclic system remains. The superposition of the side chain conformation at position C(13) shows that the conformation of the side chain at C(13) in **9b** is different from paclitaxel and docetaxel, including the orientation of the side chain relative to the core.

Table 3. Selected Torsion Angles ($^\circ$) for the C(13) Side Chain of **9b**, Paclitaxel (Molecules A and B), Docetaxel and T-Taxol

Position	9b	Paclitaxel A	Paclitaxel B	Docetaxel	T-Taxol
C(13)–O(12)–C(1')–O(13)	17.09	2	4	–6.6	0.6
C(13)–O(12)–C(1')–C(2')	–161.73	180	–177	168.0	–178.7
O(12)–C(1')–C(2')–C(3')	70.91	159	103	60.2	55.7
O(13)–C(1')–C(2')–O(14)	12.52	93	41	–2.2	–1.2
C(1')–C(2')–C(3')–N	70.60	176	179	56.4	52.4
O(14)–C(2')–C(3')–C(39)	75.42	180	–175	59.5	58.5
O(14)–C(2')–C(3')–N	–49.41	60	61	–64.6	–67.0
C(2')–C(3')–N–S(C)	–109.68	–118	–155	–141.3	–153.4
C(39)–C(3')–N–S(C)	128.47	120	83	97.3	82.8
C(3')–N–S(C)–C(45)	–77.53	–178	–178	–172.4	177.7

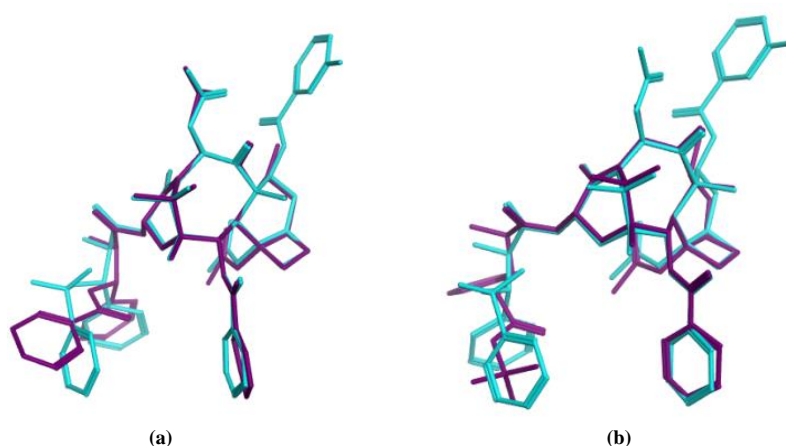


Fig. 3. (a) Superposition of the crystal structure of **9b** (blue) and paclitaxel (purple);
(b) Superposition of the crystal structure of **9b** (blue) and docetaxel (purple)

Another significant indicator concerns the distances between the centroids of the C(2) benzoyl phenyl ring and the C(3') phenyl rings, benzenesulfonamido phenyl rings. The distance between the benzene ring of C(3') of compound **9b** and the benzoyl group on C(2) is 8.7 Å (Table 4), which is close to paclitaxel (polar) A (8.9 Å), but is quite different from docetaxel and T-Taxol^[21]. The distance between the benzenesulfonyl group on the C-3'-N and the benzoyl group on C(2) is 7.2 Å, which is the same as docetaxel, but significantly different from other groups. It has been suggested that there is a hydrophobic interaction between the C(2) benzoate and the side chain aromatic groups^[22]. The hydrophobic nature of the benzoate is important for stabilizing the orientations of the C(3') substituents, and the C(2) benzoate may contribute to biological activity by

binding to a hydrophobic pocket of the tubulin protein^[3]. The changes of mutual distances may affect the hydrophobic nature of C(2) benzoate and the side chain aromatic groups, resulting in significant differences in biological activity between **9b** and paclitaxel.

In addition, in the crystal structure of **9b**, hydrogen bonds have been shown in Table 5. The N-H at the C-3'-N position forms an intermolecular hydrogen bond (N(1)-H(1A)···O(5)) with the oxygen atom in the C(4) acetyl group. The hydroxyl group at the C(1) position forms an intermolecular hydrogen bond (O(1)-H(1)···O(6)) with the oxygen atom in the four-membered ring. These hydrogen bonds may play an important role in the binding of paclitaxel compounds to receptor tubulin.

Table 4. Distances between the Centroids of the C(2) Benzoyl Phenyl Ring and the C(3') Phenyl and Benzamido Phenyl (Benzenesulfonamido Phenyl) Rings (Å) for 9b, Docetaxel, Paclitaxel and T-Taxol

Distances	9b	Docetaxel	Paclitaxel (polar)		T-Taxol
			A	B	
d1 (Å)	8.7	10.7	8.9	5.7	9.4
d2 (Å)	7.2	7.2	13.0	11.6	10.0

d1: the distances between the centroids of the C(2) benzoyl phenyl ring and the C(3') phenyl ring;

d2: the distances between the centroids of the C(2) benzoyl phenyl ring and the benzamido phenyl (benzenesulfonamide phenyl) ring or t-butyl group.

Table 5. Hydrogen Bond Distances (Å) and Bond Angles (°) for Compound 9b

Compound	D-H···A	D-H	H···A	D···A	D-H···A	Symmetry code
9b	N(1)-H(1A)···O(5)	0.86	2.15	2.96	158	-x, y-1/2, -z+2
	O(1)-H(1)···O(6)	1.06	1.83	2.80	151	-x, y-1/2, -z+1

4 BIOLOGICAL ACTIVITIES

The *in vitro* antitumor activities of the newly synthesized compounds **9a-c** were evaluated in a cytotoxicity assay employing MCF-7 (Human breast cancer cells) cell line by CCK-8 method. As shown in Fig. 4, in MCF-7 cell line, the inhibitions of compounds **9a-c** on cell survival were smaller

than paclitaxel when the concentration was 0.01~100 μM. Paclitaxel analogues obtained by introducing the hydrophobic group 3-fluorobenzoyl at C(7) and the sulfonyl group at C-3'-N did not seem to improve the biological activity significantly. According to the structural analysis of **9b**, the changes of C(7) and C(13) substituents have an effect on the overall conformation of paclitaxel analogue **9b**.

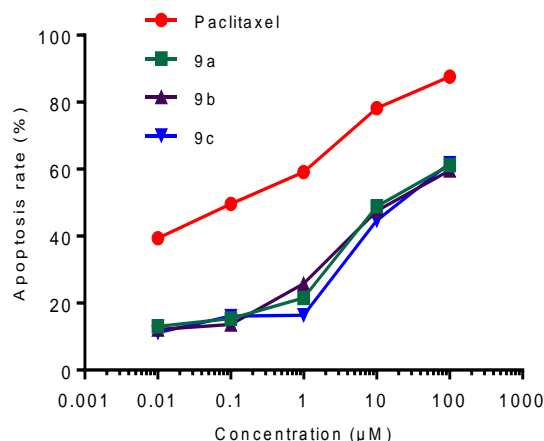


Fig. 4. Cytotoxicity assayed by CCK-8 method under growing human breast cancer cells exposed for 72 h

REFERENCES

- (1) Wani, M. C.; Taylor, H. L.; Wall, M. E.; Coggon, P.; McPhail, A. T. Plant antitumor agents. VI. Isolation and structure of taxol, a novel antileukemic and antitumor agent from *Taxus brevifolia*. *J. Am. Chem. Soc.* **1971**, 93, 2325–2327.
- (2) Liebmann, J. E.; Cook, J. A.; Lipschultz, C.; Teague, D.; Fisher, J.; Mitchell, J. B. Cytotoxic studies of paclitaxel (Taxol) in human tumour cell lines. *Br. J. Cancer*. **1993**, 68, 1104–1109.
- (3) Guenard, D.; Gueritte-Voegelein, F.; Potier, P. Taxol and taxotere: discovery, chemistry, and structure-activity relationships. *Acc. Chem. Res.* **1993**, 26, 160–167.
- (4) Panchagnula, R. Pharmaceutical aspects of paclitaxel. *Int. J. Pharmaceut.* **1998**, 172, 1–15.
- (5) Rowinsky, E. K.; Donehower, R. C.; Jones, R. J.; Tucker, R. W. Microtubule changes and cytotoxicity in leukemic cell lines treated with taxol. *Cancer Res.* **1988**, 48, 4093–4100.
- (6) Al-Farsi, A.; Ellis, P. M. Treatment paradigms for patients with metastatic non-small cell lung cancer, squamous lung cancer: first, second, and third-line. *Front. Oncol.* **2014**, 4, 157.
- (7) Lichtman, S. M. *J. Geriatr.* How I treat ovarian cancer in older women. *Oncol.* **2014**, 5, 223–229.
- (8) Ojima, I.; Wang, X.; Jing, Y. R.; Wang, C. W. Quest for efficacious next-generation taxoid anticancer agents and their tumor-targeted delivery. *J. Nat. Prod.* **2018**, 81, 703–721.
- (9) Rowinsky, E. K.; Donehower, R. C. Paclitaxel (taxol). *N. Engl. J. Med.* **1995**, 332, 1004–1014.
- (10) Ojima, I.; Borella, C.; Wu, X. Y.; Bounaud, P. Y. Design, synthesis and structure-activity relationships of novel taxane-based multidrug resistance reversal agents. *J. Med. Chem.* **2005**, 48, 2218–2228.
- (11) Bhat, L.; Liu, Y.; Victory, S. F.; Himes, R. H.; Georg, G. I. Synthesis and evaluation of paclitaxel C7 derivatives: solution phase synthesis of combinatorial libraries. *Bioorg. Med. Chem. Lett.* **1998**, 8, 3181–3186.
- (12) Georg, G. I.; Liu, Y. B.; Boge, T. C. 7-O-acylpaclitaxel analogues: potential probes to map the paclitaxel binding site. *Bioorg. Med. Chem. Lett.* **1997**, 7, 1829–1832.
- (13) Mita, A. C.; Denis, L. J.; Rowinsky, E. K. Phase I and pharmacokinetic study of XRP6258 (RPR 116258A), a novel taxane, administered as a 1-hour infusion every 3 weeks in patients with advanced solid tumors. *Clin. Cancer Res.* **2009**, 15, 723–730.
- (14) Snyder, J. P.; Nettles, J. H.; Cornett, B.; Downing, K. H.; Nogales, E. The binding conformation of Taxol in β -tubulin: a model based on electron crystallographic density. *Proc. Natl. Acad. Sci.* **2001**, 98, 5312–5316.
- (15) Ke, B.; Qin, Y.; Zhao, F. Y.; Qu, Y. Synthesis and biological evaluation of novel 3'-N-tert-butylsulfonyl analogues of docetaxel. *Bioorg. Med. Chem. Lett.* **2008**, 18, 4783–4785.
- (16) Chang, J.; Hao, Y. P.; Hao, X. D.; Lu, H. F.; Yu, J. M.; Sun, X. Synthesis and anti-HBV activity of novel 3'-N-phenylsulfonyl docetaxel analogs. *Molecules* **2013**, 18, 10189–10212.
- (17) Mastropaolo, D.; Camerman, A.; Luo, Y.; Brayer, G. D.; Camerman, N. Crystal and molecular structure of paclitaxel (taxol). *Proc. Natl. Acad. Sci.* **1995**, 92, 6920–6924.

- (18) Gabetta, B.; de Bellis, P.; Pace, R.; Appendino, G.; Barboni, L.; Torregiani, E.; Gariboldi, P.; Viterbo, D. 10-Deacetylbaaccatin III analogues from *Taxus baccata*. *J. Nat. Prod.* **1995**, 58, 1508–1514.
- (19) Xie, C. H.; Wang, D. L.; Cui, Y. M.; Lin, H. X. Crystal studies and antitumor activities of novel D-seco-taxoids derived from 1-deoxybaaccatin VI. *Chin. J. Struct. Chem.* **2019**, 38, 1511–1518.
- (20) Guéritte-Voegelein, F.; Guénard, D.; Lavelle, F.; Le Goff, M. T.; Mangatal, L. Relationships between the structure of taxol analogues and their antimitotic activity. *J. Med. Chem.* **1991**, 34, 992–99.
- (21) Alcaraz, A. A.; Mehta, A. K.; Johnson, S. A.; Snyder, J. P. The T-Taxol conformation. *J. Med. Chem.* **2006**, 49, 2478–2488.
- (22) Dubois, J.; Guenard, D.; Gueritte-Voegelein, F.; Guedira, N.; Potier, P.; Gillet, B.; Beloeil, J. C. Conformation of Taxotere® and analogues determined by NMR spectroscopy and molecular modeling studies. *Tetrahedron* **1993**, 49, 6533–6544.